

Electronic structure of the high-pressure modifications of CuCl, CuBr, and CuI

A. Blacha, N. E. Christensen,* and M. Cardona

Max-Planck-Institut für Festkörperforschung, Heisenbergstrasse 1, D-7000 Stuttgart 80, Federal Republic of Germany

(Received 12 August 1985)

The absorption spectra of edge excitons in thin films of CuCl, CuBr, and CuI have been measured as a function of hydrostatic pressure using the diamond-anvil technique. The measurements yield the pressure dependence of several exciton energies in the zinc-blende, the rhombohedral, and the tetragonal modifications of the copper halides. The experimental data are compared with band-structure calculations performed with the linear-muffin-tin-orbital method. The valence bands of the rhombohedral and tetragonal phases of the copper halides are strongly influenced by the hybridization of copper $3d$ and halogen p states. This p - d hybridization is allowed by symmetry for all points of the Brillouin zone in all modifications studied. The edge excitons are interpreted as related to direct transitions at $k=0$ between valence bands split by ligand-field and spin-orbit effects and an orbital singlet conduction band.

I. INTRODUCTION

The copper halides, CuCl, CuBr, and CuI, crystallize under ambient conditions in the zinc-blende structure. They are semiconductors, and they would, if the Cu $3d$ states were localized, have electronic structures very similar to the tetrahedrally coordinated II-VI and III-V compounds of the $A^N B^{8-N}$ type.

Considering the series Ge, GaAs, ZnSe, CuBr, for example, the $3d$ states of the first constituent play an increasing role in determining the band structure. In Ge these states can well be considered as localized core states (atomic energy level ≈ -30 eV). Already, however, in GaAs they have moved up in energy by 10 eV, and their hybridization with the valence-band top affects the gap.¹ Proceeding further in the series, this effect becomes more important, and in CuBr the Cu $3d$ states even overlap in energy with the halogen p states with which they strongly hybridize. Therefore, the band structures of the copper halides are very different from those of the other compound semiconductors.^{1,2}

For the zinc-blende structure this d - p hybridization is allowed at all points in \mathbf{k} space, and it causes the top of the valence band to move up in energy.¹⁻⁴ Consequently, the energy gaps are smaller than they would be if the hybridization did not occur. This shift (≈ 1 eV) causes the fundamental gap of the copper halides to be of a direct nature. In contrast, the gaps found in the NaCl structure (which is a high-pressure modification) are indirect, and the reason is⁴ that in that structure the hybridization is symmetry forbidden at the zone center. Other important consequences of the Cu- d halogen- p hybridization have been found. The spin-orbit splitting Δ_0 of the uppermost valence band in CuCl is negative, whereas^{2,3,5} it is positive (but small) in CuBr and CuI. Also, the small magnitude^{4,6-8} of the deformation potentials of gaps and valence-state splittings related to hydrostatic and uniaxial strains can be attributed to the strong d - p hybridization. The pressure-induced changes in the d - p interaction tend to compensate for the changes in the Cu- p halogen- p in-

teractions.⁷ No such compensation takes place in the group-IV, -III-V, and -II-VI semiconductors,⁷ and they therefore have deformation potentials that are much larger than those of the copper halides.^{7,8}

The copper halides undergo a number of structural phase transitions under pressure.⁹ We shall examine here, also by theoretical methods,¹⁰⁻¹² some of these, which have previously been studied by x-ray-diffraction measurements^{9,13-18} for temperatures ranging from room temperature to the melting point. The sequence of the phase transitions is nearly the same for CuCl, CuBr, and CuI. CuBr and CuCl transform from the zinc-blende structure (CuCl II, CuBr III) to a tetragonal structure (CuCl IV, CuBr V) at about 5 GPa, and further to the NaCl structure (CuCl V, CuBr VI) for pressures above ~ 10 GPa. CuI transforms from the zinc-blende structure (CuI III) first to a rhombohedral structure (CuI IV) at 1.4 GPa, and then at 4 GPa it changes to a tetragonal modification (CuI V). For pressures above 10 GPa, CuI is supposed to be stable in the NaCl structure (CuI VIII).

The published lattice parameters of all high-pressure modifications of the copper halides are listed in Table I. Reliable data for the atomic coordinates in the high-pressure phases are available only for CuI. According to Meisalo and Kalliomäki,^{9,18} it is characteristic of the pressure-induced phase transitions of CuI that the iodine sublattice remains a nearly ideal or only slightly deformed fcc lattice. The copper atoms occupy different sites with either tetrahedral coordination (in the case of the zinc-blende, rhombohedral, and tetragonal phases) or octahedral coordination (for the NaCl-type structure). For the tetragonal structure of CuBr and CuCl the Bravais lattices were determined, but no reliable data for the atomic positions within the unit cell have been published. However, Raman measurements¹⁹ and optical-absorption measurements (see below) are compatible with the assumption that the tetragonal phases of CuCl, CuBr, and CuI have the same or rather similar structures.

In this paper we present optical-absorption spectra of thin films of CuCl, CuBr, and CuI for pressures between

TABLE I. Lattice parameters a and c of the tetragonal (tet.) phases CuCl IV, CuBr V, and CuI V and the rhombohedral (rhomb.) phase CuI IV. The lattice constants of the zinc-blende structures at 298 K and zero pressure are 5.4057 Å for CuCl II, 5.6905 Å for CuBr V, and 6.0427 Å for CuI III.

Compound	a (Å)	c (Å)	Pressure	Reference
CuCl IV	5.21	4.61	5.5	9
	5.27	4.688	4.4	14
	4.89	5.23	5.5	16
	6.376	6.468	5.0	18
CuBr V	5.4	4.75	5.5	9
	6.695	6.715	5.0	18
CuI V (tet.)	4.02	5.70	6.5	9
	4.039	5.650	6.6	18
CuI VI ^a (rhomb.)	4.164	20.41	1.6	9
	4.143	20.3	2.24	18

^a a and c refer to a hexagonal unit cell (Refs. 9 and 18).

0 and 10 GPa. The samples had a thickness of about 3000 Å. For such thin samples the transmission of light is always larger than 10%, even for photon energies above the fundamental absorption edge. Therefore, several excitons, related to holes in different valence bands, can be observed in the absorption spectra. Thus absorption measurements on thin films give more detailed information about the electronic band structure than investigations of the fundamental absorption edge of bulk crystals as performed by Ves *et al.*⁴ for the high-pressure phases of the copper halides. Our experiments yield the dependence on hydrostatic pressure of the energies of excitons related to holes in the two highest valence bands. Data have been obtained for the zinc-blende phases and for the rhombohedral and tetragonal modifications. The high-pressure phases of the copper halides with NaCl structure are known to have an indirect energy gap. Consequently, the absorption spectra of thin samples in the NaCl modification do not show any significant structure.

For comparison with our experimental data, we have performed band-structure calculations on the basis of the linear muffin-tin orbital (LMTO) method.¹⁰ The electronic properties of the zinc-blende phases of the copper halides have already been studied in the past.^{2-4,6,7} Band-structure calculations for the NaCl-type phases based on the LMTO method have been discussed by Ves *et al.*⁴ in connection with measurements of the absorption edge. In this paper we also present self-consistent, relativistic band-structure calculations for the tetragonal phases performed with the LMTO method using the local approximation to the density-functional formalism.^{11,12}

The outline of this paper is as follows: In Sec. II the experimental details are discussed. The experimental results are presented in Sec. III. In Sec. IV they are compared with the results of the band-structure calculations.

II. EXPERIMENT

In order to perform optical transmission measurements at high pressures we used a gasketed diamond-anvil cell^{6,20,21} with a 4:1 methanol-ethanol mixture as the pressure-transmitting fluid. The samples, thin films of about 3000 Å thickness, were evaporated from pieces of

single crystals onto one of the diamond anvils. The measurements were performed at room temperature and at 100 K.

At room temperature the samples experience nearly hydrostatic strains as the transmitting fluid seems to flow smoothly around them.⁶ However, at temperatures lower than 150 K the fluid hardens and the pressure is not transmitted hydrostatically to the sample, which experiences a mixture of hydrostatic and shear stress.⁶ For the samples under consideration, the shear component of the strain tensor is proportional to the hydrostatic pressure p in the pressure-transmitting fluid if $p \leq 3$ GPa. If $p \geq 3$ GPa the uniaxial component of the pressure acting on the sample becomes small, possibly due to plastic flow.⁶ At sufficiently high pressures the conditions become relatively hydrostatic, even at low temperatures.

In the case of CuCl and CuBr, pressure-induced phase transitions take place at pressures above 5 GPa. Thus experiments on the high-pressure phases of CuBr and CuCl under relatively hydrostatic conditions can be performed at low temperatures. Measurements at low temperatures are useful because some details of the band structure, such as the spin-orbit splittings, cannot be resolved at room temperature. In the case of CuI the spin-orbit-split bands are well separated and measurements at low temperatures are not required to resolve the spin-orbit splitting. This is a fortunate circumstance since the first phase transformation of CuI takes place below 2 GPa, a pressure at which—at low temperature—considerable uniaxial components would exist.

For the optical transmission measurements we used either a xenon arc or a halogen lamp as light sources and a SPEX double monochromator with photon-counting electronics and a resolution of 0.5 Å. The pressure inside the cell was determined with a ruby-fluorescence manometer.²⁰ The absorption spectra were obtained by comparing the transmission spectra of the system with and without the sample.

III. EXPERIMENTAL RESULTS

Typical absorption spectra of thin films of CuCl and CuBr measured at 100 K as described in the preceding

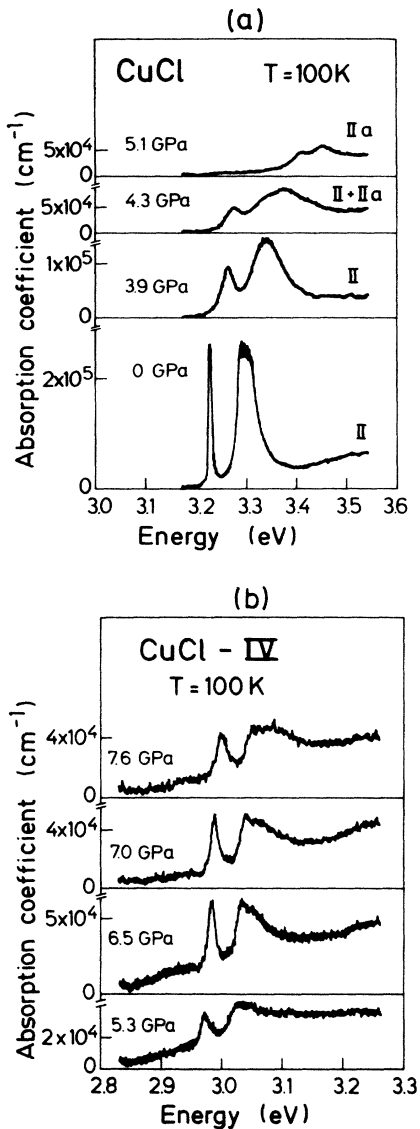


FIG. 1. Absorption spectra of 3000-Å-thick CuCl films for various pressures at 100 K; (a) zinc-blende structure and (b) tetragonal structure.

section are shown in Figs. 1 and 2 for cell pressures up to 8 GPa. Absorption spectra of CuI measured at room temperature are given in Fig. 3 for pressures below 6 GPa.

The absorption spectra in Figs. 1–3 show two or three peaks related to the creation of excitons by the incident light. The energies of these peaks are plotted in Figs. 4–6 as a function of the measured pressure. Pressure-induced phase transitions appear in Figs. 4–6 as discontinuities of the energy-versus-pressure curves. The data for the zinc-blende phases have already been published in Ref. 6.

IV. DISCUSSION

The transition pressures obtained from Figs. 4–6 are listed in Table II, together with other data in the literature which were obtained by means of Raman spectroscopy and x-ray diffraction. The observed transitions are as-

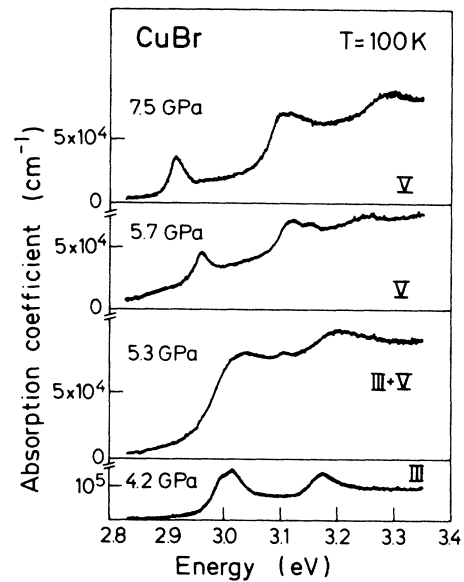


FIG. 2. Absorption spectra of 3000-Å-thick CuBr films for various pressures at 100 K. Data for phases III and V are shown.

signed to different phases as investigated by x-ray diffraction.^{9,18} The various values for the transition pressures of CuCl and CuBr from the zinc-blende to the tetragonal structures (CuCl II→CuCl IV, and CuBr III→CuBr IV), and those for CuI from the zinc-blende (CuI III) to the rhombohedral (CuI IV) and the tetragonal structure (CuI V), are in reasonable agreement. However, there is a large scatter of the published values for the transition pressures to the NaCl structure (CuCl V, CuBr VI, CuBr VIII). In this work we have estimated these pressures as the highest pressures at which exciton peaks are observed. As the phases with NaCl structure have an indirect gap,⁴ one does not expect exciton peaks in their absorption edges. Therefore, if there is a coexistence of the tetragonal and

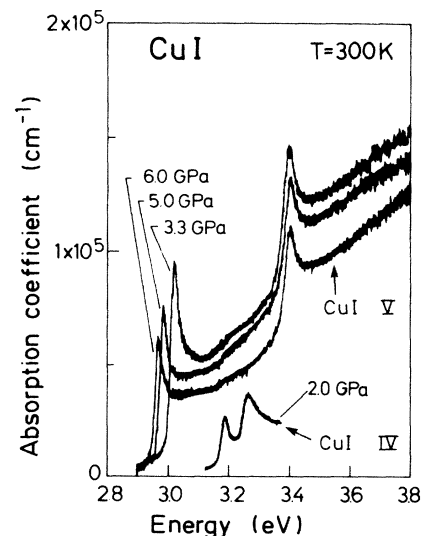


FIG. 3. Absorption spectra of 3000-Å-thick CuI films for various pressures at 100 K. Phases IV and V are shown.

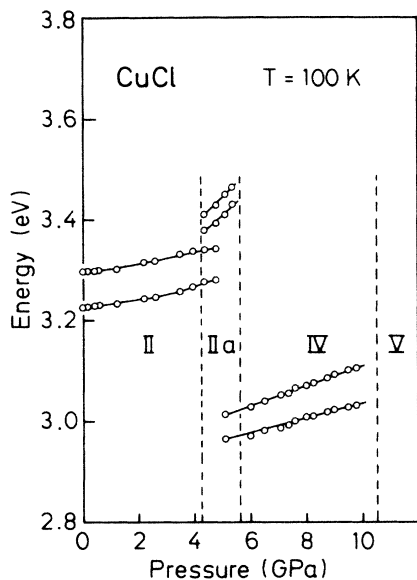


FIG. 4. Exciton energies of CuCl as a function of hydrostatic pressure at 100 K. The pressure range of the different phases (CuCl II, IIa, IV, and V) is marked by dashed lines.

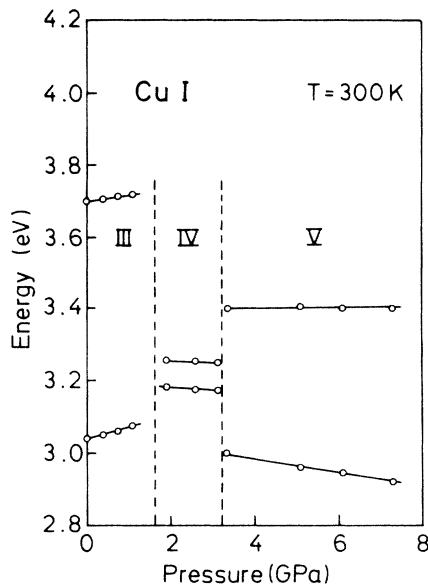


FIG. 6. Exciton energies of CuI as a function of hydrostatic pressure at 300 K. The pressure range of the different phases (CuI III, IV, and V) is marked by dashed lines.

the NaCl-type phases for a finite range of pressures, uncertainties in the determination of the transition pressure to the NaCl structure from the transmission spectra arise. The same problem exists for the Raman experiments (see Table II) since the zone-center phonons of crystals with NaCl structure are not Raman active and thus cannot be observed.

In order to assign the absorption peaks in Figs. 1–3 to different allowed optical transitions between the valence and conduction bands, it is helpful to compare the ener-

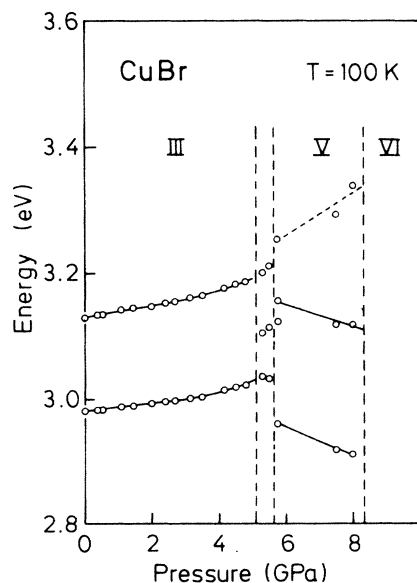


FIG. 5. Exciton energies of CuBr as a function of hydrostatic pressure at 100 K. The pressure ranges where the different structures (CuBr III, V, and VI) are stable are marked by dashed lines.

gies of the absorption peaks with those of the fundamental absorption edges of the high-pressure modifications (see Ref. 4). In Table III we have listed the energies of the observed exciton peaks of the (tetragonal and rhombohedral) high-pressure phases (Figs. 4–6). We have called the energy of the lowest peak E_1 and that of the second peak E_2 . In Table III, E_1 and E_2 are compared with the energy gaps E_g published in Ref. 4. The derivatives of E_1 , E_2 , and E_g with respect to pressure are also given in Table III. For CuCl and CuI, E_1 is only about 30–50 meV larger than E_g , and the pressure derivative of E_1 has the same sign and magnitude as the pressure derivative of E_g . Thus, in this case, the absorption peaks observed for thin-film samples can be safely assigned to edge excitons related to electrons in the lowest conduction band and holes in the highest valence bands (see below). Consequently, from the spectra in Figs. 1 and 3, we can determine the pressure dependence of the energy difference between the conduction bands and the two highest valence bands of the high-pressure modifications of CuCl and CuI (except for the NaCl-type phases). In the absorption spectra of CuCl we found in a double-peak structure at around 3.4 eV for pressures between 4.5 and 5.5 GPa. These peaks are possibly related to the so-called IIa phase of CuCl,^{13,23} although there have been controversies about the existence of such a phase; its appearance may be dependent on sample preparation.^{14,23} As the presumable CuCl IIa films are not well characterized, we do not want to discuss this point any further.

The interpretation of the exciton spectra of the high-pressure phases of CuBr (Fig. 2) presents some problems. At room temperature CuBr has a tetragonal structure for pressures between 5 and 9 GPa (see Table II). Our optical-absorption measurements performed at 100 K clearly show that there is a phase transition at 5 GPa (Fig.

TABLE II. Transition pressures in GPa for copper halides at room temperature. The nomenclature for the different phases is chosen according to Ref. 9.

Reference	CuCl			CuBr			CuI	
	IIa	IV	V	V	VI	IV	V	VIII
This work ^a	4.2	5.0	~10.5	5.0	9.0	1.4	3.3	> 7.5
19 ^b		5.0	~10.5	5.0	9.0	1.5	4.0	> 15
9 ^c		5.2	6.0	5.0	6.6	1.4	4.1	8.0
13 ^d	4.2	5.5	10.0					
19 ^e						1.4	3.9	
22 ^f	4.0	6.0	9.0					
14 ^g		4.4	8.2					
15 ^h		5.5	10.5					
4 ⁱ		5.0	9.0	5.0	7.5	1.8	4.6	9.0
18 ^j		4.8	8.5	4.9	6.8	1.48	3.8	9.2

^aThe transition pressures have been determined for increasing applied pressures in the case of CuCl and CuBr and for decreasing pressure in the case of CuI.

^bRaman measurements.

^cX-ray measurements.

^dX-ray and electrical conductivity measurements.

^eRaman measurements.

^fElectrical conductivity.

^gX-ray and electrical conductivity.

^hX-ray measurements.

ⁱOptical absorption of bulk samples.

^jX-ray measurements.

2). However, the only excitons observed for pressures between 5 and 9 GPa are about 400 meV above the energy E_g of the edge observed in bulk samples (2.45 eV at 6 GPa at room temperature). Although the phase diagram of CuBr has not been investigated for temperatures below 300 K, it is reasonable to assume that the measurements above room temperature can be extrapolated smoothly to low temperatures. If this is done, the excitons found at 100 K for pressures above 5 GPa cannot be the edge excitons of the tetragonal phase. Their energies are much too high in comparison to the energy gap measured for the tetragonal phase CuBr V extrapolated to low temperatures. Thus, if the tetragonal phase CuBr V does exist also at low temperatures, one must explain why exciton peaks close to the bulk absorption edge of the tetragonal phase have not been found. On the other hand, a different sequence of pressure-induced phase transitions at low temperatures cannot be completely ruled out. To clarify this point, we tried to measure the optical absorption of a thin film of CuBr at room temperature as a function of pressure. Unfortunately, the sample always pulled loose from the diamond anvil and broke for pressures above 4 GPa. Thus we could not measure any exciton spectra of the tetragonal phase of CuBr at room temperature. Under these circumstances a definite interpretation of the exci-

tonic spectra of CuBr in Fig. 2 for pressures above 5 GPa is difficult. However, it should be mentioned that Raman measurements¹⁹ are compatible with the assumption that CuBr, as well as CuCl and CuI, have the same tetragonal structure at low temperatures for pressures above 5 GPa.

In the following we discuss the excitonic spectra of the tetragonal phases of CuCl and CuI and compare them with LMTO (Ref. 10) band-structure calculations based on the local-density approximation for exchange and correlation.^{11,12} We have performed the calculations for different volumes of the tetragonal unit cells of CuCl and CuI and the same c/a ratio. Additionally, we calculated the electronic pressure as a function of volume.^{24–27} In this way we were able to calculate the first-order pressure coefficients of the energy bands and the bulk modulus $B = -dp/d \ln V$.

In Fig. 7 the calculated band structure for the tetragonal phase of CuI is shown. The calculations were performed for the lattice parameters $a = 4.02$ Å and $c = 5.70$ Å of the tetragonal unit cell at 6.5 GPa given in Refs. 9 and 18 (also see Table I). We assumed that this phase of CuI has PbO structure^{9,18} (Fig. 8), i.e., that there are two copper and two iodine atoms per unit cell. The coordinates of these atoms with respect to the axis a_1, a_2, c of the tetragonal unit cell (Fig. 8) are

TABLE III. Energy gap E_g and exciton energies E_1, E_2 in eV ($E_1 < E_2$, see Figs. 4–6) of the tetragonal phases of the copper halides (CuCl IV, CuBr V, CuI V) at 6 GPa and the rhombohedral phase CuI IV at 3 GPa. The numbers in parentheses are the pressure coefficients of the energies in meV/GPa.

	CuCl IV	CuBr V	CuI V	CuI IV
E_g^a	2.92 (21)	2.49 (7.4)	2.92 (–11)	3.09 (–14.8)
E_1^b	2.97 (14)	2.95 (–17)	2.95 (–18)	3.17 (–8)
E_2^b	3.03 (20)	3.15 (–22)	3.4 (0)	3.25 (–3)

^aReference 4, room-temperature data.

^bThis work, measured at 100 K (CuCl, CuBr) or at 300 K (CuI).

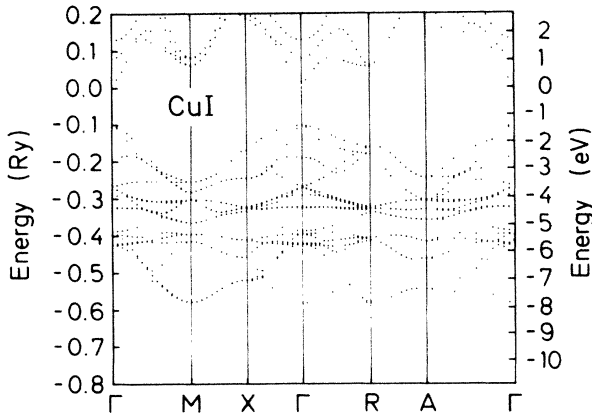


FIG. 7. LMTO band structure (self-consistent) of the tetragonal phase of CuI assumed to have PbO structure with the lattice parameters $a=4.02$ Å and $c=5.7$ Å, which correspond to 6.5 GPa (Table I, Fig. 8). Spin-orbit coupling has been neglected, but the other relativistic effects are included.

$$\begin{aligned}
 \text{atom 1 (I): } & (0,0,0), \\
 \text{atom 2 (Cu): } & (0.5,0,\bar{z}), \\
 \text{atom 3 (Cu): } & (0,0.5,\bar{z}), \\
 \text{atom 4 (I): } & (0.5,0.5,0.5),
 \end{aligned} \tag{1}$$

with $\bar{z} \approx 0.28$.^{9,18} Furthermore, we have assumed that $c/a=1.42$, independent of volume. The LMTO method requires the structure to be close packed and, therefore, the band calculations were made by introducing four “empty spheres,” i.e., atomic spheres with no nuclear charge. This is also necessary for the zinc-blende structure (see, e.g., Ref. 30 and references therein).

The LMTO calculations yields for the energy gap between the highest valence band and the lowest conduction band a value which is about half the experimental gap (Table III, Fig. 7). A similar discrepancy has been found for the zinc-blende phases.^{4,8} It is a consequence^{28,1,8} of the local-density approximation (LDA). Nevertheless, the LDA method normally yields reliable values for the shifts

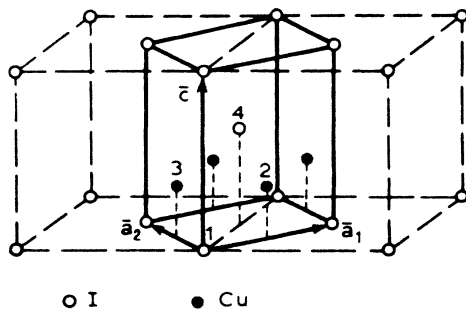


FIG. 8. Unit cell of the tetragonal PbO structure of CuI V (Refs. 9, 18, and 37). The tetragonal unit cell is spanned by the vectors \mathbf{a}_1 , \mathbf{a}_2 , and \mathbf{c} . The positions of the atoms within the unit cell are given in (1).

of energy bands when the volume is varied^{8,29,30} The bands of Fig. 7 can be regarded as a “folded” version of those of zinc-blende structure,⁴ the folding along the $\Gamma-X$ direction corresponding to the doubling of the primitive cell. According to Fig. 7 the lowest gap of the tetragonal phase should be direct. This is in agreement with the experiment.⁴ The LMTO calculation predicts that this gap should be at the Γ point of the Brillouin zone.

The band structure shown in Fig. 7 does not include effects of the spin-orbit coupling. We have also performed some calculations with spin-orbit coupling at selected points of the Brillouin zone. For the spin-orbit splitting Δ_0 of the uppermost valence band at Γ , we calculated 0.47 eV assuming $a=4.02$ Å and $c=5.70$ Å (i.e., corresponding to the experimental pressure 6.5 GPa). This value agrees with the separation of the two absorption maxima in Fig. 3 (0.465 eV at 6.5 GPa, see Fig. 6). Thus the energy difference between the edge excitons in Fig. 7 can be identified with the spin-orbit splitting of the highest valence band at the Γ point of the Brillouin zone. The top of the valence band is first split by the tetragonal crystal and ligand field (~ 1 -eV splitting). The resulting orbitally doubly degenerate top state is then split by the spin-orbit interaction, giving rise to the observed doublet.

In Table IV, LMTO data for the following quantities calculated for three different sets of lattice parameters a and c , with $c/a \approx 1.42$, are listed:

- The spin-orbit splitting Δ_0 of the uppermost valence band at the Γ point.
- The energy differences E_{g1} and E_{g2} between the highest valence band and the lowest and next-lowest conduction bands.
- The calculated electronic pressure p .

TABLE IV. Tetragonal phase of CuI (CuI V): pressure p , spin-orbit splitting Δ_0 of the highest valence band at Γ , and energy gaps E_{g1}, E_{g2} between the highest valence band and the two lowest conduction bands, calculated for the PbO structure (Fig. 8) for different lattice parameters a and c ($c/a=1.42$). The self-consistent calculations have been performed using the relativistic LMTO method. The linear pressure coefficients and the volume derivatives of p , Δ_0 , E_{g1} , and E_{g2} determined for $a=4.02$ Å and $c=5.70$ Å (experimentally realized at 6.5 GPa) are also given.

	a (Å)		
	4.02	4.17	4.32
p (GPa)	14.7	5.76	0.44
Δ_0 (eV)	0.468	0.394	0.330
E_{g1} (eV) ^a	1.3	1.16	1.08
E_{g2} (eV) ^a	2.17	2.26	2.28
$d\Delta_0/dp$ (meV/GPa)	8		
$d\Delta_0/d \ln V$ (eV)	-0.68		
dE_{g1}/dp (meV/GPa)	16		
$dE_{g1}/d \ln V$ (eV)	-1.36		
dE_{g2}/dp (meV/GPa)	-10		
$dE_{g2}/d \ln V$ (eV)	0.85		
$B = dp/d \ln V$ (GPa)	-85		

^aSpin-orbit splitting of the highest valence band taken into account.

The values of the linear pressure coefficients and volume derivatives of Δ_0 , E_{g1} , E_{g2} , and p calculated for the lattice parameters $a=4.02$ Å and $c=5.70$ Å are also given. The pressure coefficient calculated for the spin-orbit splitting Δ_0 of the tetragonal phase of CuI is 8 meV/GPa. This is about a factor of 2 smaller than the experimental value (18 meV/GPa, see Table III). (Note, in this context that volume dependences are calculated assuming a fixed c/a ratio.) According to the LMTO calculations the pressure coefficient of the direct energy gap E_{g1} between the highest valence band and the lowest conduction band should be positive (+16 meV/GPa, Table IV). The experimental result is $dE_{g1}/dp = -18$ meV/GPa instead. For the pressure coefficient of the direct energy gap E_{g2} between the highest valence band and the second-lowest conduction band, the LMTO calculation yields a negative value $dE_{g2}/dp = -10$ meV/GPa. Perhaps the local-density approximation leads to the incorrect order for the lowest two conduction bands.

As can be seen from Table IV, the calculated pressure p acting on the tetragonal phase of CuI with lattice parameters $a=4.02$ Å and $c=5.70$ Å is 14.7 GPa. This is about a factor of two larger than the experimental value of 6.5 GPa (Table I). We believe that this deviation arises from uncertainties in the calculation of the pressure. Discrepancies between the calculated values for the pressure coefficients of Δ_0 , E_{g1} , and E_{g2} can possibly arise from the arbitrary assumption that the ratio c/a is independent of volume. Experimental information about this ratio versus pressure is not available. Nevertheless, our LMTO band-structure calculations, based on the crystal structure proposed in Refs. 9 and 18 [PbO structure, Eq. (1), Table I], are qualitatively consistent with the experimental findings.

The interpretation of the excitonic spectra of the tetragonal phase of CuCl (CuCl IV, Fig. 1) by means of band-structure calculations is more difficult than in the case of CuI because a variety of inconsistent sets of lattice parameters have been published for CuCl IV. Reliable experimental data for the positions of the atoms within the tetragonal unit cell are not available.^{9,18,31} We have assumed that the tetragonal phase of CuCl also has the PbO structure, as does the tetragonal phase of CuI [Eq. (1), Fig. 8]. The lattice parameters given for CuCl IV in Refs. 4 and 18 are inconsistent with our assumption of the similarity of the band structures of CuCl IV and CuI V. The parameters from Refs. 9 and 14, however, are consistent with that assumption, provided one assigns the parameter a (Table I) to $\sqrt{2}$ times the length of the basis vectors $\mathbf{a}_1, \mathbf{a}_2$ of the tetragonal unit cell of the PbO structure (Fig. 8). Otherwise, the volume of the tetragonal phase would be larger than the volume of the zinc-blende phase. On the basis of this assumption, we have calculated the band structure of the tetragonal phase of CuCl. The result, calculated for the lattice parameters $a=3.64$ Å and $c=4.61$ Å (Refs. 9 and 14), is given in Fig. 9. According to Ref. 9, these lattice constants correspond to 5.5 GPa. A comparison of Figs. 7 and 9 shows that the structure of the conduction bands is similar for CuCl and CuI. In agreement with the experiment, the LMTO calculations suggest that the lowest-energy gap of the tetragonal phase of

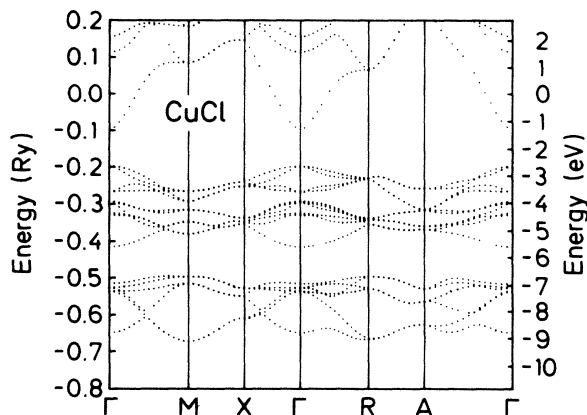


FIG. 9. Scalar-relativistic (i.e., spin-orbit coupling is omitted) LMTO band structure (self-consistent) of the tetragonal phase of CuCl calculated for the PbO structure (see Fig. 8) with $a=3.64$ Å and $c=4.61$ Å corresponding to 5.5 GPa.

CuCl should also be direct and at the Γ point of the Brillouin zone. The calculated pressure coefficient of the lowest conduction band is positive for CuCl IV and negative for the second-lowest conduction band, a situation analogous to that found for CuI V.

In Table V some numerical results of the LMTO band structure of the tetragonal phase of CuCl are listed: the spin-orbit splitting Δ_0 of the uppermost valence band at the Γ point, the direct energy gaps E_{g1} and E_{g2} between the highest valence band and the lowest two conduction bands, the pressure p , and the linear pressure coefficients of Δ_0 , E_{g1} , and E_{g2} . Also, in this case we have assumed that c/a does not change with pressure. The calculated

TABLE V. Tetragonal phase of CuCl: pressure p , spin-orbit splitting Δ_0 of the highest valence band at Γ , and energy gaps E_{g1}, E_{g2} between the highest valence band and the two lowest conduction bands, calculated with the LMTO method for the PbO structure (Fig. 8) for different lattice parameters a and c ($c/a=1.25$). The linear pressure coefficients and the volume derivatives of p , Δ_0 , E_{g1} , and E_{g2} for $a=3.64$ Å and $c=4.61$ Å (experimentally realized at 5.5 GPa) are also given.

	a (Å)		
	3.64 ^a	3.80	3.96
p (GPa)	34.6	15.9	5.0
Δ_0 (eV)	0.010	0.021	0.031
E_{g1} (eV)	1.66	1.36	0.84
E_{g2} (eV)	4.15	4.24	4.35
$d\Delta_0/dp$ (meV/GPa)	-0.58		
$d\Delta_0/d \ln V$ (eV)	0.086		
dE_{g1}/dp (meV/GPa)	16		
$dE_{g1}/d \ln V$ (eV)	-2.3		
dE_{g2}/dp (meV/GPa)	-5		
$dE_{g2}/d \ln V$ (eV)	0.7		
$B = dp/d \ln V$ (GPa)	147		

^aWe assume that the values for a published in Refs. 9 and 14 (see Table I) refer to the slightly deformed fcc unit cell of the halogen sublattice (see Fig. 8). The values for a in this table designate the length of vectors $\mathbf{a}_1, \mathbf{a}_2$ (Fig. 8) which span the basis of the tetragonal unit cell of the PbO structure.

value for the pressure which is necessary to compress the tetragonal unit cell with PbO structure to a size experimentally realized at 5.5 GPa ($a=3.68$ Å, $c=4.61$ Å referred to the tetragonal unit cell) is 34.6 GPa. This large discrepancy between theory and experiment (29.1 GPa) suggests that the crystal-structure determinations of the tetragonal phase of CuCl should be carefully checked.^{18,31} Nevertheless, the experimental pressure coefficient of the direct energy gap E_{g1} is 21 meV/GPa (Table III), while the LMTO calculation yields 16 meV/GPa (Table V), a rather acceptable result. This calculation, however, depends critically on the value of the bulk modulus used to convert the calculated volume coefficient into a pressure coefficient. Above we used the calculated $B=147$ GPa. From x-ray measurements Piermarini *et al.*¹⁴ have obtained $B=87$ GPa, while Skelton *et al.*¹⁵ have determined $B=200$ GPa for CuCl IV, two values which encompass the calculated one. The band calculation yields the right order of magnitude for the spin-orbit splitting of the highest valence band at Γ [LMTO, $\Delta_0=0.01$ eV for $a=3.68$ Å, $c=4.61$ Å; experiment, $\Delta_0=0.05$ eV for 5.5 GPa under the assumption that it corresponds to the two peaks in Fig. 1(b)]. The discrepancy is not surprising in view of the strong compensation between Cl $3p$ and Cu $3p$ contributions.¹ However, the calculated sign of the pressure coefficient of Δ_0 disagrees with experiment, if our assignment is correct.

It is of interest to discuss in which way the electronic structure of the tetragonal phases of the copper halides is influenced by the p - d hybridization, particularly whether the p - d hybridization is symmetry allowed for all points of the Brillouin zone (especially at Γ). We discuss this question for the highest valence band. The PbO structure has inversion symmetry (point group D_{4h}), which may exclude a hybridization of p and d states because p and d functions have different parity. This is just the reason why p - d hybridization does not exist at the Γ point for NaCl-type crystals. However, the primitive cell of the tetragonal PbO phase of the copper halides consists of four atoms: two copper atoms and two halogen atoms (Fig. 8). In this case one can construct wave functions with a definite parity at $k=0$ using appropriate combinations of p and d orbitals placed at each of the two equivalent atoms. Hence the p (and also the d) functions can lead to either even or odd parity depending on whether their bonding or antibonding combination is considered: The valence bands of the tetragonal phases of the copper halides (with PbO structure) must be strongly influenced by the p - d hybridization in the entire Brillouin zone. In a LCAO description the wave functions of the highest valence states at the Γ point must have the form

$$\begin{aligned}\psi_{\text{I}}^{\pm} &= \alpha(|p_x\rangle_{1\mp} + |p_x\rangle_{4\pm}) + \beta(|d_{zx}\rangle_{2\pm} + |d_{zx}\rangle_{3\pm}), \\ \psi_{\text{II}}^{\pm} &= \alpha(|p_y\rangle_{1\mp} + |p_y\rangle_{4\pm}) + \beta(|d_{zy}\rangle_{2\pm} + |d_{zy}\rangle_{3\pm}), \\ \psi_{\text{III}} &= \gamma(|p_z\rangle_{1\mp} + |p_z\rangle_{4\pm}) + \delta(|d_{3z^2-r^2}\rangle_{2\pm} + |d_{3z^2-r^2}\rangle_{3\pm}),\end{aligned}\quad (2)$$

where $\alpha^2 + \beta^2 = 1$, $\gamma^2 + \delta^2 = 1$. The arabic digits refer to the numbering of the atoms in Fig. 8. The states $|p_x\rangle$, $|p_y\rangle$, \dots , $|d_{zx}\rangle$, \dots are linear combinations of p or d orbitals at equivalent atoms, where the coordinates x, y, z

refer to the directions of the vectors $\mathbf{a}_1, \mathbf{a}_2, \mathbf{c}$ in Fig. 8. The highest valence band is doubly degenerate at the Γ point (neglecting spin-orbit coupling). Thus, the highest valence band corresponds to the states ψ_{I} and ψ_{II} in (2). The state ψ_{III} is separated from ψ_{I} and ψ_{II} by the ligand field splitting. This splitting should be of the order of 1 eV (Figs. 7 and 9). The admixture coefficients α, β or γ, δ can be used to characterize the strength of the p - d hybridization of the valence bands. We have estimated α and β for the PbO-type phase of CuCl and CuI from our LMTO calculations. The results are $\alpha^2=0.45$ and $\beta^2=0.55$ for CuCl and $\alpha^2=0.61$ and $\beta^2=0.39$ for CuI. Obviously, the admixture of d states to the p states is larger for the tetragonal phase of CuCl than for the tetragonal phase of CuI, the same trends³²⁻³⁴ as found for the zinc-blende phases for which the wave functions of the highest valence states can be written as a linear combination of halogen p orbitals and copper d states,

$$\psi_x = \alpha_0 |p_x\rangle_{\text{halogen}} + \beta_0 |d_{yz}\rangle_{\text{Cu}} \quad (3)$$

(and cyclic permutations of x, y, z), with $\alpha_0^2 + \beta_0^2 = 1$. Representative values for α_0^2 are 0.25 for CuCl, 0.36 for CuBr, and 0.5 for CuI.^{2,3,35-37} Similar trends exist for the pressure coefficients of the admixture coefficients $\alpha, \beta, \alpha_0, \beta_0$. Our LMTO calculations show that the admixture of Cu $3d$ states to the highest valence states of the tetragonal phases of CuI and CuCl decreases with increasing pressure. The same effect was found for the zinc-blende phases of the copper halides.^{35,36}

In the case of the rhombohedral phase of CuI, the p - d hybridization is also allowed by symmetry for all points of the Brillouin zone, this time because of the lack of inversion symmetry (point group C_{3v} , space group C_{3v}^5). Band-structure calculations for this phase have not yet been performed. Before starting additional calculations, one should, however, have more reliable data for the crystal structures of the high-pressure phases. It would also be desirable to have experimental data for the atomic coordinates and for the variation of c/a with pressure.

V. CONCLUSIONS AND SUMMARY

The high-pressure modifications of the copper halides show sharp edge excitons in the photon-energy region around 3 eV where the edge excitons of the low-pressure zinc-blende phases also occur. The interpretation of these excitons in terms of electronic energy bands is hampered by uncertainties in the crystallographic structure of these high-pressure phases. For the tetragonal phase of CuI (phase V), however, the tetragonal PbO structure seems to be well established. This may also be the case for the tetragonal phase of CuCl (phase IV), although further structure determinations are required. We have thus performed relativistic LMTO calculations for these phases of CuI and CuCl under the assumption that the atomic positions in the case of CuCl are the same within the unit cell as those determined experimentally for CuI. We have also calculated the dependence of these band structures on volume (and pressure). The calculated absorption edges are lower than the experimental exciton energies, as expected for LMTO calculations. The pressure coefficient

of the edge calculated for the tetragonal phase of CuCl, however, agrees reasonably with the experimental one. For this calculation the theoretically determined bulk modulus (147 GPa) was used in view of the large discrepancies (87–200 GPa) among experimental determinations of bulk moduli for this phase of CuCl.

In the case of CuI the calculated pressure coefficient of the gap has a sign opposite of that found experimentally. This discrepancy can be removed if the order of the two lowest conduction bands as found in the LMTO calculation is reversed.

The phase diagram of CuBr is only partially known.

Our experimental data taken at low temperatures (≈ 100 K) are difficult to relate to models assuming the structure to be tetragonal between 5 and 9 GPa, as observed above 300 K. We do observe a pressure-induced transition to a structure V (Fig. 5) existing between 5.7 and ≈ 8.2 GPa, but the exciton spectra are quite different from those observed for the tetragonal phases of CuI and CuCl.

ACKNOWLEDGMENTS

We thank W. Dieterich, H. Hirt, M. Siemers, and P. Wurster for technical support.

*Permanent address: Physics Laboratory I, Technical University of Denmark, DK-2800 Lyngby, Denmark.

- ¹G. B. Bachelet and N. E. Christensen, *Phys. Rev. B* **31**, 879 (1985).
- ²M. Cardona, *Phys. Rev.* **129**, 69 (1963).
- ³A. Goldmann, *Phys. Status Solidi B* **81**, 9 (1977).
- ⁴S. Ves, D. Glötzel, H. Overhof, and M. Cardona, *Phys. Rev. B* **24**, 3073 (1981).
- ⁵K. Shindo, A. Morita, and H. Kamimura, *J. Phys. Soc. Jpn.* **20**, 2054 (1965).
- ⁶A. Blacha, S. Ves, and M. Cardona, *Phys. Rev. B* **27**, 6346 (1983).
- ⁷A. Blacha, H. Presting, and M. Cardona, *Phys. Status Solidi B* **126**, 11 (1984).
- ⁸N. E. Christensen, *Phys. Status Solidi B* **123**, 281 (1984); **125**, K59 (1984).
- ⁹V. Meisalo and M. Kalliomäki, *High Temp.-High Pressures* **5**, 663 (1973).
- ¹⁰O. K. Andersen, *Phys. Rev. B* **12**, 3060 (1975).
- ¹¹P. Hohenberg and W. Kohn, *Phys. Rev.* **136**, B864 (1964); W. Kohn and L. J. Sham, *ibid.* **140**, A1133 (1965).
- ¹²L. Hedin and B. I. Lundquist, *J. Phys. C* **4**, 2064 (1971).
- ¹³N. R. Serebryanaya, S. V. Popova, and A. P. Rusakov, *Fiz. Tverd. Tela (Leningrad)* **17**, 2772 (1975) [*Sov. Phys.—Solid State* **17**, 1843 (1976)].
- ¹⁴G. J. Piermarini, F. A. Maurer, S. Block, A. Jayaraman, T. H. Geballe, and G. W. Hull, *Solid State Commun.* **32**, 275 (1979).
- ¹⁵E. F. Skelton, A. W. Webb, F. J. Rachford, P. C. Taylor, S. C. Yu, and I. L. Spain, *Phys. Rev. B* **21**, 5289 (1980).
- ¹⁶E. F. Skelton, F. J. Rachford, A. W. Webb, S. C. Yu, and I. L. Spain, in *Physics of Solids Under Pressure*, edited by J. S. Schilling and R. N. Skelton (North-Holland, Amsterdam, 1981).
- ¹⁷E. F. Skelton, S. B. Quadri, A. W. Webb, R. G. Ingalls, and J. M. Tranquada, *Phys. Lett.* **94A**, 441 (1983).
- ¹⁸M. Kalliomäki, Report No. HU-P-D34, University of Helsinki, 1982 (unpublished).
- ¹⁹A. Blacha and M. Cardona (unpublished).
- ²⁰G. F. Piermarini, S. Block, J. D. Barnett, and R. A. Forman, *J. Appl. Phys.* **46**, 2774 (1975).
- ²¹S. Hawke, K. Syassen, and W. Holzapfel, *Rev. Sci. Instrum.* **45**, 1548 (1974).
- ²²O. Brafman and M. Cardona, *Phys. Rev. B* **15**, 1081 (1977).
- ²³C. W. Chu, A. P. Rusakov, S. Huang, S. Early, T. H. Geballe, and C. Y. Huang, *Phys. Rev. B* **18**, 2116 (1978).
- ²⁴D. G. Pettifor, *Commun. Phys.* **1**, 141 (1976).
- ²⁵R. M. Nieminen and C. H. Hodges, *J. Phys. F* **6**, 573 (1976).
- ²⁶A. R. Mackintosh and O. K. Andersen, in *Electrons at the Fermi Surface*, edited by H. Springford (Cambridge University Press, Cambridge, 1979).
- ²⁷N. E. Christensen and V. Heine (unpublished).
- ²⁸D. R. Haman, *Phys. Rev. Lett.* **42**, 662 (1979).
- ²⁹J. A. Vergés, D. Glötzel, M. Cardona, and O. K. Andersen, *Phys. Status Solidi B* **113**, 519 (1982).
- ³⁰N. E. Christensen, *Phys. Rev. B* **30**, 5753 (1984).
- ³¹K. J. Smolander, *J. Phys. C* **16**, 3673 (1983).
- ³²L. Kleinman and K. Mednick, *Phys. Rev. B* **20**, 2487 (1979).
- ³³A. Zunger and M. Cohen, *Phys. Rev. B* **20**, 1189 (1979).
- ³⁴S. Y. Ren, R. E. Allen, J. D. Dow, and I. Lefkowitz, *Phys. Rev. B* **25**, 1205 (1982).
- ³⁵A. Blacha, M. Cardona, N. E. Christensen, and S. Ves, *Solid State Commun.* **43**, 183 (1982).
- ³⁶A. Blacha, M. Cardona, N. E. Christensen, S. Ves, and H. Overhof, in *Proceedings of 16th International Conference on the Physics of Semiconductors, Montpellier, 1982* [*Physica* **117&118B**, 63 (1983)].
- ³⁷J. Smolander, Report No. HU-P-D17, University of Helsinki, 1980 (unpublished).